*Tikrit Journal of Pure Science (2024) 29 (1): 107-118*
**Doi:** https://doi.org/10.25130/tjps.v29i1.1451

TJPS

IASJ
المجلات الاكاديمية العراقية

**Tikrit Journal of Pure Science**
*ISSN: 1813 – 1662 (Print) --- E-ISSN: 2415 – 1726 (Online)*

**Journal Homepage:** http://tjps.tu.edu.iq/index.php

# The Effect of Laser Energy on the Structural, Optical and Electrical Properties of CdO Nanomaterials Generated Using (PLD) Technology, and Fabrication a Gas Sensor

[1]Basil S. Ahmed, [2]Sabri Jasim Mohammad, [3]Ghuson H. Mohammed
*[1,2]Department of Physics - College of Education for pure sciences - Tikrit University - Iraq*
*[3]Department of Physics - College of Sciences - University of Baghdad - Iraq*

**Keywords:** PLD, Cadmium oxide, Gas Sensor, $NH_3$, thin films.

**ARTICLEINFO.**

**Article history:**

| | |
|---|---|
| **-Received:** | **25 July 2023** |
| **-Received in revised form:** | **23 Aug. 2023** |
| **-Accepted:** | **24 Aug. 2023** |
| **-Final Proofreading:** | **24 Feb. 2024** |
| **-Available online:** | **25 Feb. 2024** |

**Corresponding Author*:**
**basil.s.ahmed@st.tu.edu.iq**



**ABSTRACT**

In this study, cadmium oxide (CdO) nanoparticles were synthesized using laser produced plasma technology with varying energy levels (300, 400, 500, and 600) mJ. These nanoparticles were deposited as a thin layers on glass surfaces (at a rate of 100 pulses). They were examined structurally and optically using a Scanning Electron Microscope (FESEM), X-Ray spectrophotometer (XRD), Atomic Force Microscope (AFM), and UV-visible spectrophotometer. The energy gap of the films varied from (1.5 eV) to (2.1 eV). We note that the energy gap decreases with increasing laser intensity. The FESEM and AFM images show a large anisotropy in the structure as the roughness varies with different energies. X-ray investigations indicated the presence of many crystals and a variation in the crystal structure of the film. The Figure of Merit (F.O.M) diagram revealed that the optimal energy was (400 mJ). A gas sensor for gas ($NH_3$) was created, and the impact of increasing gas ratios and temperature on gas sensitivity over time was investigated.

*Tikrit Journal of Pure Science (2024) 29 (1): 107-118*
**Doi:** https://doi.org/10.25130/tjps.v29i1.1451

TJPS

# تأثير طاقة الليزر على الخصائص التركيبية والبصرية والكهربائية لجسيمات (CdO) النانوية المتولدة باستخدام تقنية (PLD)، وتصنيع مستشعر غازي

باسل صباح احمد[1]، صبري جاسم محمد[2]، غصون حميد محمد[3]
[1,2] قسم الفيزياء – كلية التربية للعلوم الصرفة – جامعة تكريت – العراق
[3] قسم الفيزياء – كلية العلوم – جامعة بغداد – العراق

**الملخص**

في هذه الدراسة ، تم تصنيع جسيمات اوكسيد الكادميوم النانوية (CdO) باستخدام تقنية البلازما المنتجة بالليزر بمستويات طاقة مختلفة (٣٠٠ ، ٤٠٠ ، ٥٠٠ ، ٦٠٠) مللي جول. ترسبت هذه الجسيمات النانوية على شكل طبقات رقيقة على الأسطح الزجاجية (بمعدل ١٠٠ نبضة). ثم تم فحصها هيكليًا وبصريًا باستخدام مسح المجهر الإلكتروني (FESEM)، ومقياس الطيف الضوئي بالأشعة السينية (XRD)، ومجهر القوة الذرية (AFM) ومقياس الطيف المرئي للأشعة فوق البنفسجية. تراوحت فجوة الطاقة في الأغشية من (١,٥ الكترون فولت) إلى (٢,١ الكترون فولت). نلاحظ أن فجوة الطاقة تتناقص مع زيادة شدة الليزر. تُظهر صور FESEM و AFM تباينًا كبيرًا في الهيكل حيث تختلف الخشونة باختلاف الطاقات. أشارت قياسات الأشعة السينية إلى وجود العديد من البلورات وتباين في التركيب البلوري للغشاء. أظهر الرسم البياني للنتائج الأفضل (F.O.M)أن الطاقة المثلى كانت (٤٠٠ ملي جول). تم تصنيع مستشعر للغاز ($NH_3$)، وتم التحقق من تأثير زيادة نسب الغاز ودرجة الحرارة على حساسية الغاز بمرور الوقت.

**الكلمات المفتاحية:** PLD ، أكسيد الكادميوم، مستشعر الغاز، الامونيا، الأغشية الرقيقة.

## 1. Introduction

Cadmium oxide has a low electrical resistance due to the presence of cadmium atoms at interstitial locations or through oxygen gaps. It has a high absorption coefficient, enabling it to be utilized in solar systems to increase the efficiency of photovoltaic cells [1,2]. It is a semiconductor with the periodic table group (II-VI) [3], and a cubic crystal structure and a face-centered cubic (FCC) unit cell, similar to the structure of a crystal of sodium chloride (NaCl) [4,5]. CdO is a transparent conductive oxides (TCO) family semiconductor material [6,7,8]. It has unusual properties such as a large energy gap extending between (1.5 - 2.4 eV) [9], and apparent transparency. It has high reflectivity at the red region of the electromagnetic spectrum [10], high carrier mobility [11], and high electrical conductivity similar to negative-type metals (n-type) [4,9], as well as good fluorescence and many applications in electro-optical devices and display devices [12]. CdO is a cadmium compound that is soluble in acids and ammonia salts but not water or alkalis [13]. Pulsed Laser Deposition (PLD) technology is considered one of the best technologies used in this field, because it gives the largest number of thin films in record time, by controlling the number of pulses and laser energy. Cadmium oxide has distinctive properties that enable it to be used in many different scientific applications and technological [11,13]. The aim of this research is to make a gas sensor ($NH_3$) and study the effect of gas ratios and temperature on the sensitivity values.

## 2- Preparation Method

The target was prepared in powder form and pressed into a disc with a diameter of (1 cm) and a thickness of (0.5 cm), at a pressure of (6 Tons) and a period of (20 min), after which cadmium oxide nanoparticles were prepared using laser-induced plasma technology with a Nd: YAG laser at (1064 nm) and for various energies (300, 400, 500, 600) mJ. These nanoparticles were deposited in thin layers on glass surfaces using (at a rate of 100 pulses). It was then examined using FESEM, XRD, AFM, and UV-visible spectrophotometer.

XRD was used to determine the crystalline structure and grain size of the CdO films produced utilizing PLD techniques. The grain size (D) was calculated using Scherrer's equation [14].

$$D\ (\text{Å}) = k\lambda/\beta\cos\theta \quad \text{------------------------------------------------} \quad (1)$$

(D) signifies the crystallite size, (k) is the Scherer's constant (k = 0.9), λ denotes the X-ray wavelength (1.540 Å), and (β) denotes the Full Width at Half Maximum (FWHM) of the peaks at the diffracting angle (θ) from the Bragg's angle location. The optical properties were investigated using a twin beam UV-Vis spectrophotometer (MetertechSP8001, Taiwan).

Tauc's equation for direct transition was used to visually estimate the optical band gap [15].

$\alpha h\upsilon = K (h\upsilon - Eg)^{n}$ ---------------------------------------------------- (2)

Where, (α) is the absorption coefficient, (K) is the proportionality constant, (hυ) represents the energy of the incident photon, and ($E_g$) is the band gap energy, where (n = ½) for indirect band gap and (n = 2) for direct band gap.

Figure of merit to judge the performance transparent – conducting of films, figure of merit need to be estimated this was found from the following equation.

$F.O.M = \frac{\alpha}{\sigma}$ --------------------------------------------------- (3)

Where σ: is the film conductivity, and α: is absorption coefficient [16].

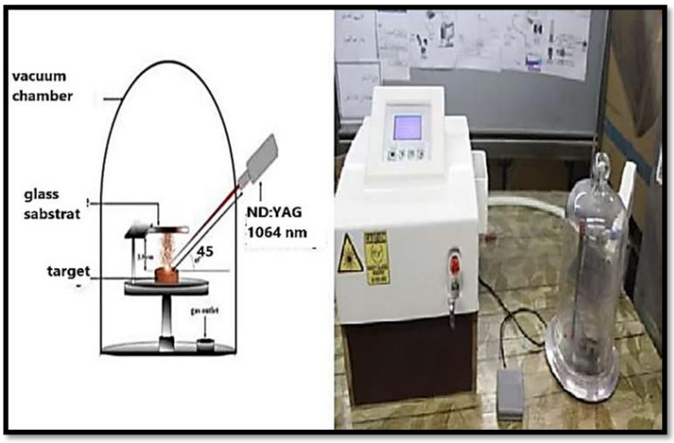


Figure (1). The pulsed laser device as well as a schematic design of the pulsed laser deposition system.

## 3- Results and discussion

### *3-1 XRD analyses*

The X-ray diffraction analyses revealed that all of the thin films were made with a polycrystalline structure. XRD patterns of the CdO composite films with varied energies are shown in Fig.2. These patterns include peaks centered at 2θ equals to: (28.72), (32.94), (34.80), (38.24), (51,21), (55.24), (57.19), (62.35), (65.84), and (69.15) corresponding to Miller indices (101), (111), (200), (110), (220), (013), (311) and (211). The angles 2θ which equals to: (28.72), (32.94), (38.24), (51,21), (55.24), (57.19), (65.84), and (69.15), belong to (CdO). These results coincide with Card data (No: ICDD 01-075-0592), but not with Miller indices: (002), (010), and (110). The angles (31.84), (34.80), and (62.35) pertain to $Cd_2$, these results are consistent with Card data (No: ICSD 98-009-8179). The figure clearly shows that the CdO thin film has a polycrystalline structure and is preferentially oriented along (111), (200), and (220) crystallographic orientations. It was discovered that when the energy was (400 mJ), the intensity of the peaks rose in a different manner for certain peaks, but when the energy was raised to (500 mJ and 600 mJ), the strength of the peaks decreased. This is in agreement with [17]. CdO compounds are generally a cubic crystal system, while $Cd_2$ has a hexagonal crystal system. The film may be observed to be orientated preferentially along (111) crystallographic orientations as well as (200), and (220). This reflects the uniformity of the film material and the relative purity of the target employed, whereas several peaks emerged when the energies were raised, such as (110) This is due to increased evaporation rates and corresponds with [18].

 **TJPS**

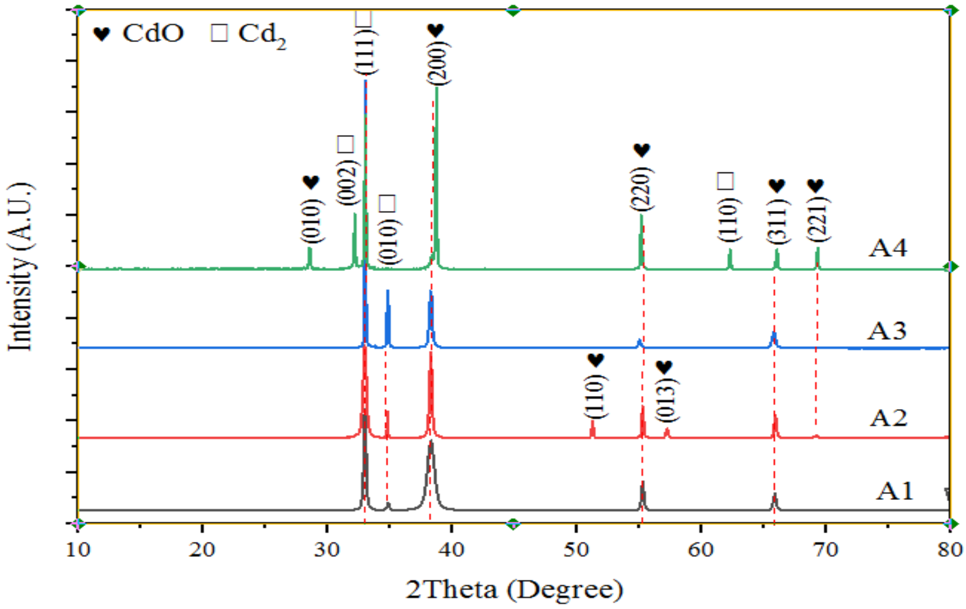


Figure (2). XRD patterns of the prepared thin films at different energies ($A_1$ = 300 mJ, $A_2$ = 400 mJ, $A_3$= 500 mJ, $A_4$ = 600 mJ )

Table 1. Results obtained by XRD measurements performed on samples with different energies

| Energy (mJ) | Material | Exp. Pos. (2θ°) | FWHM Left (2θ°) | hkl | G.S (nm) | Crystal system | Reference code |
|---|---|---|---|---|---|---|---|
| 300 mJ | CdO | 32.9478 | 0.216 | (111) | 39.8 | Cubic | ICDD 01-075-0592 |
| | $Cd_2$ | 34.8023 | 0.117 | (010) | 76.1 | Hexagonal | ICSD 98-009-8179 |
| | CdO | 38.2461 | 0.543 | (200) | 15.7 | Cubic | ICDD 01-075-0592 |
| | CdO | 55.242 | 0.177 | (220) | 53.2 | Cubic | ICDD 01-075-0592 |
| | CdO | 65.841 | 0.196 | (311) | 50.4 | Cubic | ICDD 01-075-0592 |
| 400 mJ | CdO | 32.934 | 0.3 | (111) | 28.4 | Cubic | ICDD 01-075-0592 |
| | $Cd_2$ | 34.7681 | 0.0673 | (010) | 141.1 | Hexagonal | ICSD 98-009-8179 |
| | CdO | 38.2309 | 0.216 | (200) | 40.4 | Cubic | ICDD 01-075-0592 |
| | CdO | 51.2174 | 0.142 | (110) | 65.7 | Cubic | ICSD 98-016-1837 |
| | CdO | 55.2488 | 0.144 | (220) | 65.9 | Cubic | ICDD 01-075-0592 |
| | CdO | 57.1913 | 0.2176 | (013) | 43.1 | Cubic | ICDD 01-075-0592 |
| | CdO | 65.8798 | 0.1116 | (311) | 91 | Cubic | ICDD 01-075-0592 |
| | CdO | 69.1559 | 0.3435 | (221) | 28.7 | Cubic | ICDD 01-075-0592 |
| 500 mJ | CdO | 32.9756 | 0.2708 | (111) | 31.5 | Cubic | ICDD 01-075-0592 |
| | $Cd_2$ | 34.8118 | 0.19 | (010) | 45.7 | Hexagonal | ICSD 98-009-8179 |
| | CdO | 38.2328 | 0.2448 | (200) | 35.5 | Cubic | ICDD 01-075-0592 |
| | CdO | 54.9962 | 0.2448 | (220) | 37.8 | Cubic | ICDD 01-075-0592 |
| | CdO | 57.053 | 0.29 | (013) | 32.1 | Cubic | ICDD 01-075-0592 |
| | CdO | 65.7769 | 0.3264 | (311) | 29.8 | Cubic | ICDD 01-075-0592 |
| | CdO | 69.2516 | 0.19 | (221) | 53 | Cubic | ICDD 01-075-0592 |
| 600 mJ | CdO | 28.7218 | 0.2753 | (010) | 30.7 | Cubic | ICSD 98-016-1837 |
| | $Cd_2$ | 31.8453 | 0.236 | (002) | 36.2 | Hexagonal | ICSD 98-009-8179 |
| | CdO | 33.0251 | 0.177 | (111) | 49 | Cubic | ICDD 01-075-0592 |
| | CdO | 38.3033 | 0.295 | (200) | 29.3 | Cubic | ICDD 01-075-0592 |
| | CdO | 55.2687 | 0.236 | (220) | 39.3 | Cubic | ICDD 01-075-0592 |
| | $Cd_2$ | 62.3507 | 0.2556 | (110) | 37.5 | Hexagonal | ICSD 98-009-8179 |
| | CdO | 65.9293 | 0.3736 | (221) | 25.9 | Cubic | ICDD 01-075-0592 |
| | CdO | 69.187 | 0.3736 | (221) | 26.4 | Cubic | ICDD 01-075-0592 |

### *3-2 AFM Analyses*

AFM was used to investigate the topography of surface structures. Figure (3) represents AFM images of different energies of CdO thin films.

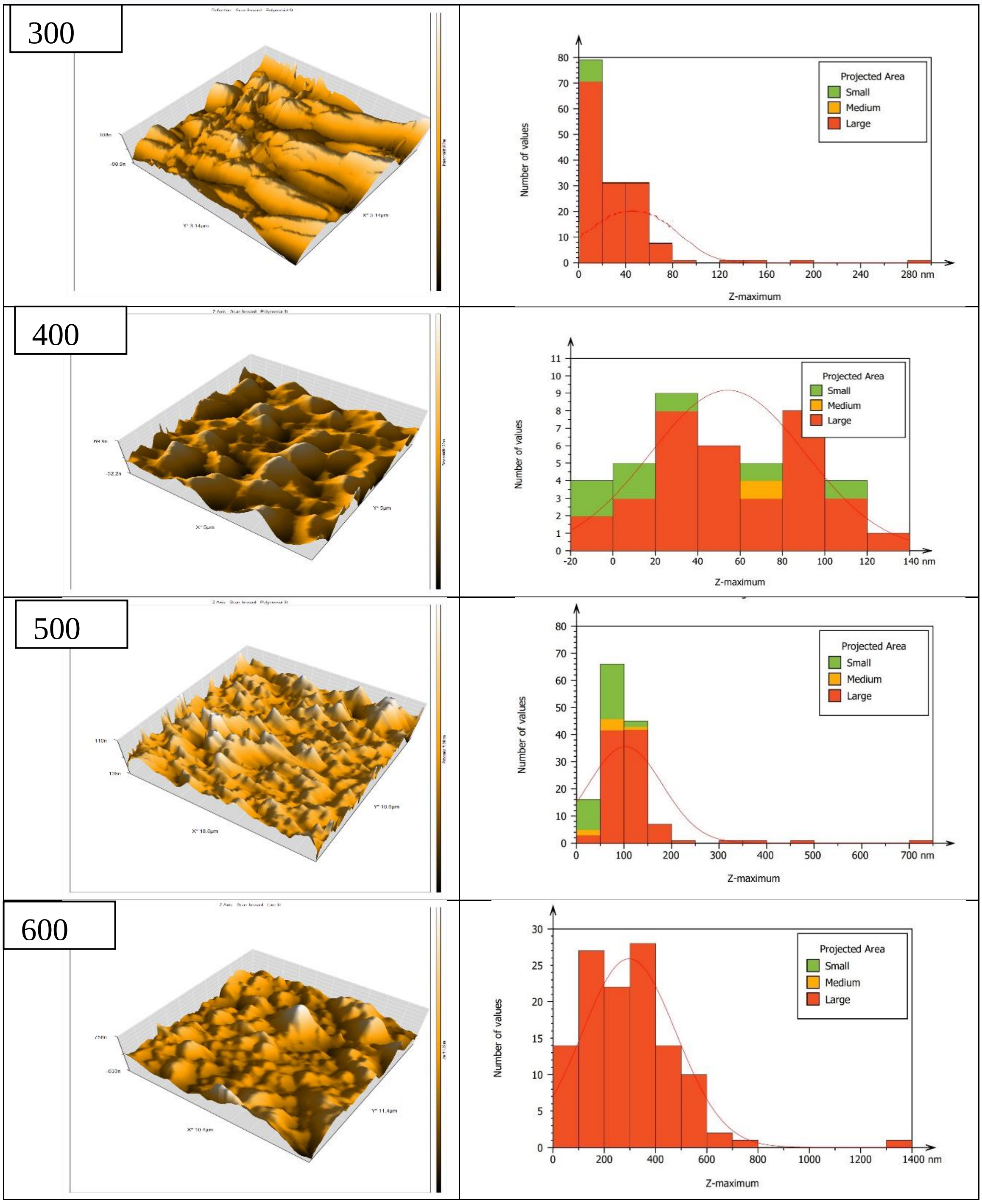


Figure (3). The structural properties of CdO after plasma bombardment with energy (300 mJ -600 mJ).

Table (2). AFM parameters (average diameter, average thickness) of the CdO thin films. Thin films were deposited on a glass substrate by laser pulses.

| Laser (mJ Energy) | Avg. Diameters(nm) | Avg. thickness(nm) |
|---|---|---|
| 300 | 47.19 | 22.14 |
| 400 | 54.22 | 26.04 |
| 500 | 109.13 | 37.61 |
| 600 | 297.00 | 108.17 |

The diameter of the grains increases as the power of the laser beam increases. This increase is due to two factors: higher laser power generates big particles, and increasing laser energy causes microscopic particles to unite, resulting in the soldered process and increased numbers. Surface roughness and grain diameter will increase as a consequence [19].

***3-3 FESEM Analyses***

The morphology of the CdO nanoparticles created by PLD technique was examined using FESEM technique. The SEM pictures confirmed that the produced particles had the nature and form of nanoparticles, and that the nanoparticles agglomerate, as shown in Fig (4). The increased surface areas and surface energy of may be attributable to the presence of certain large grains and CdO agglomeration. Because of its enormous surface area to volume ratio. We notice the appearance of nanoclusters and agglomeration of the thin films in a spherical shape, which makes it more sensitive to gas in order to increase the interaction area.

Spherical structures are very important in gas sensors because they result in high surface energy and high surface tension, and they are very important in photodetectors and gas sensors [16].

*Tikrit Journal of Pure Science (2024) 29 (1): 107-118*
**Doi:** https://doi.org/10.25130/tjps.v29i1.1451 **TJPS**

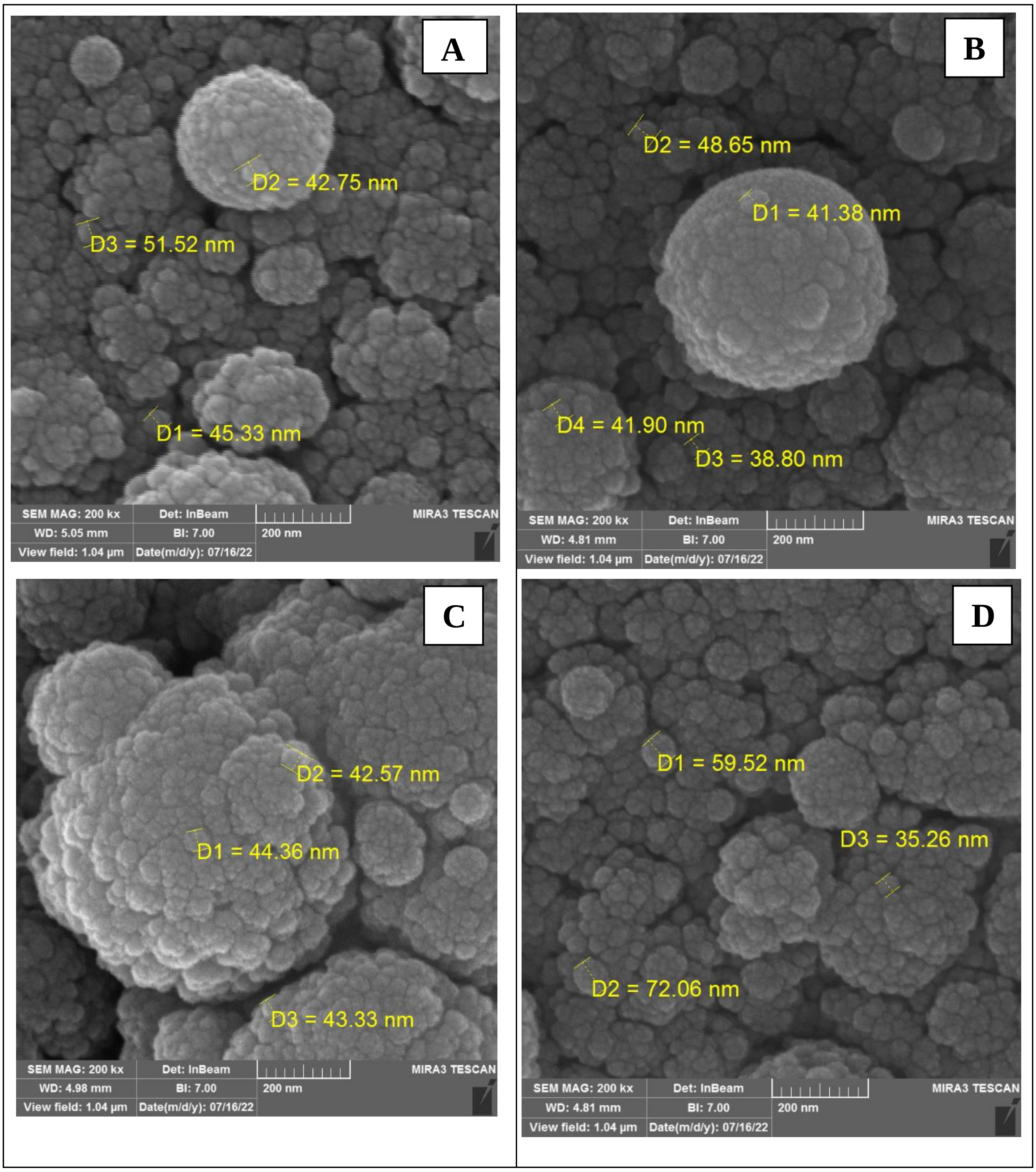


Figure (4). FESEM images of CdO synthesized by PLD technique: A) 300 mJ, B) 400 mJ, C) 500 mJ, D) 600 mJ.

### *3-4 UV-Visible Analysis*

It is observed that the diameter of the grains increases in tandem with the power of the laser energy. This increase is due to two factors: increasing the laser power leads to the growth of large granules, and increasing the laser power stimulates the small granules to cohesion, which leads to the welding process that generates huge granules with an increase in grain diameter and surface roughness. As we mentioned earlier, this is confirmed by Table (3) .

*Tikrit Journal of Pure Science (2024) 29 (1): 107-118*
**Doi:** https://doi.org/10.25130/tjps.v29i1.1451



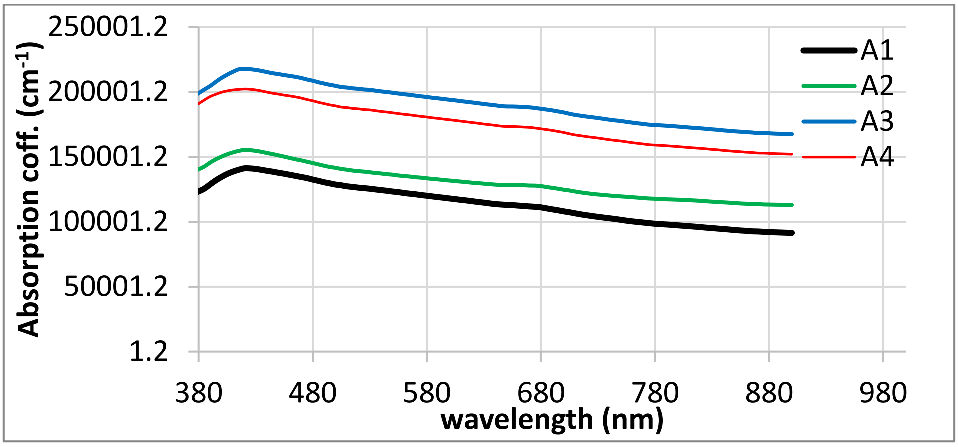


Figure (5). The relationship between the wavelength and the absorbance coefficient for CdO thin films

Figure (5) shows the variation of the absorption coefficient (α) as a function of wavelength for CdO thin films with various laser pulse intensities. The results show that the absorption coefficient is larger ($\alpha > 10^4$ $cm^{-1}$) in these films, which suggests that they are directly electronic. It is happening. Moreover, we also notice that the absorbance valuesdecrease slightly with increasing wavelength and the absorbance rate increases with increasing energies with a slight variation at energy (500 mJ) with symbol ($A_3$). This is in agreement with [20].

Figure (6) show different laser pulsed energies. The optical energy gap, also known as the gap for direct electronic transitions permitted in CdO thin films, was determined using the Tauc equation [21] with (r = ½) by drawing a straight line tangent to the curve between $(\alpha h\nu)^2$ and (hν). The incident photon, continuing the straight line until it meets the photon's energy axis at ($(\alpha h\nu)^2 = 0$). Figure 6 depicts the optical energy gap for direct transfer of CdO films. Photon absorption increases as laser power increases owing to a reduction in the value of the energy gap and the formation of localized states in the band gap. (See Figure 6, and Table 3). These findings were shown to be compatible with [22].

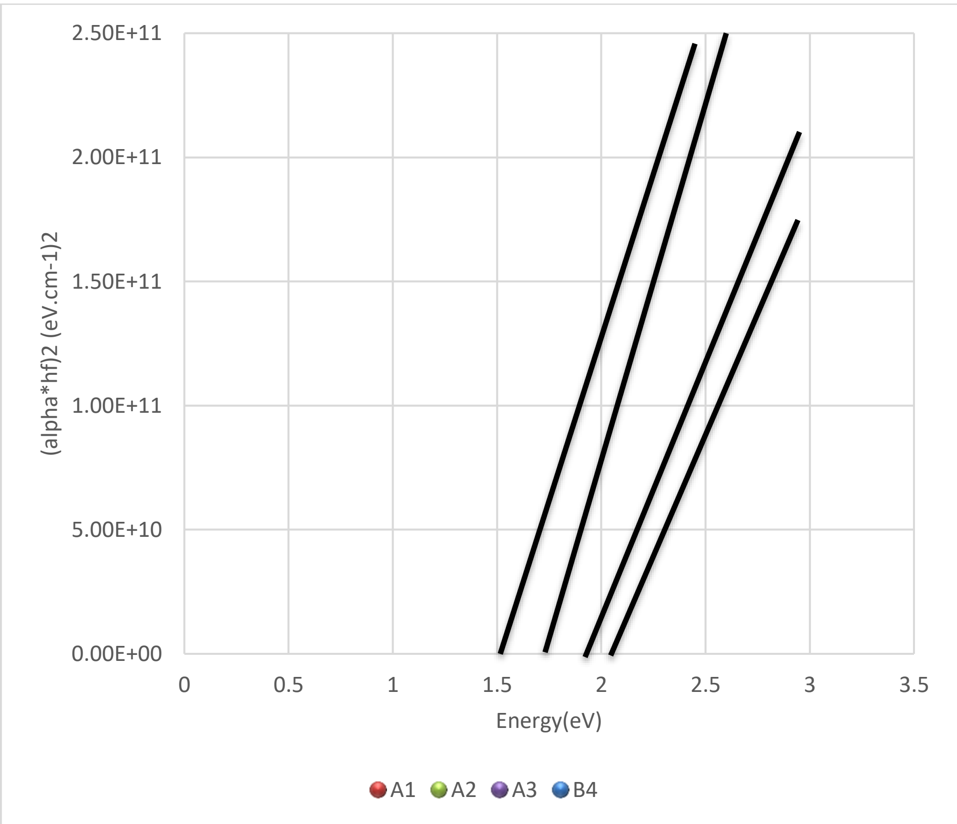


Figure (6). The Variation of $(\alpha h\upsilon)^2$with (hυ) (CdO) nanoparticles at different laser pulsed energy: $A_1$=300 mJ ,

$A_2$=400 mJ, $A_3$=500 mJ, $A_4$=600 mJ

Table (3). For each of the multiple energies employed for PLD-mediated film deposition, the energy gap was

| Energy | $R_H$ ($cm^{-3}C^{-1}$) | N ($cm^{-3}$) | ϙ (o.cm)$^{-1}$ | μ ($cm^2V^{-1}s^{-1}$) | Conductivity Type |
|---|---|---|---|---|---|
| 300 mj | -1.30E+02 | -4.80E+16 | 1.80E+01 | 2.35E+03 | n |
| 400 mj | -1.03E+02 | -9.73E-03 | 1.47E+01 | 1.51E+03 | n |
| 500 mj | -9.44E+01 | -5.30E-03 | 2.99E+01 | 2.82E+03 | n |
| 600 mj | -1.57E+01 | -2.12E-02 | 3.10E+01 | 4.87E+02 | n |

determined using UV-Vis spectra of (CdO) nanoparticles and nanoparticle size measurements.

Table (4). Hall effect measurements for (CdO) thin films with different energy

| Sample | Energy (mJ) | Energy gap (eV) | Particles size(nm) |
|---|---|---|---|
| $A_1$ | 300 | 2.1 | 42.12 |
| $A_2$ | 400 | 1.9 | 46.73 |
| $A_3$ | 500 | 1.7 | 58.07 |
| $A_4$ | 600 | 1.5 | 97.45 |

### *3-5 Hall Effect Measurements*

It is clear from Table (4) that all samples have a negative Hall coefficient (i.e. n-type conductivity). The carrier concentration ($n_H$) and the type of conductivity in addition to their Hall mobility (μH) were determined with different pulsed laser energy for CdO thin films using four point probe resistance technology (Van Der Pauw) and Hall measurement with application of (0.25 T) magnetic field. The results show that increasing the value of the laser power leads to a movement of the Hall kinetics and a significant decrease in the carrier concentration.

### *3-6 Figure of Merit*

After applying equation (3) and extracting the values of (F.O.M) we notice from the figure (7) and the table (5) that energy (500 mJ) is the best, so it was chosen to make the gas sensor.

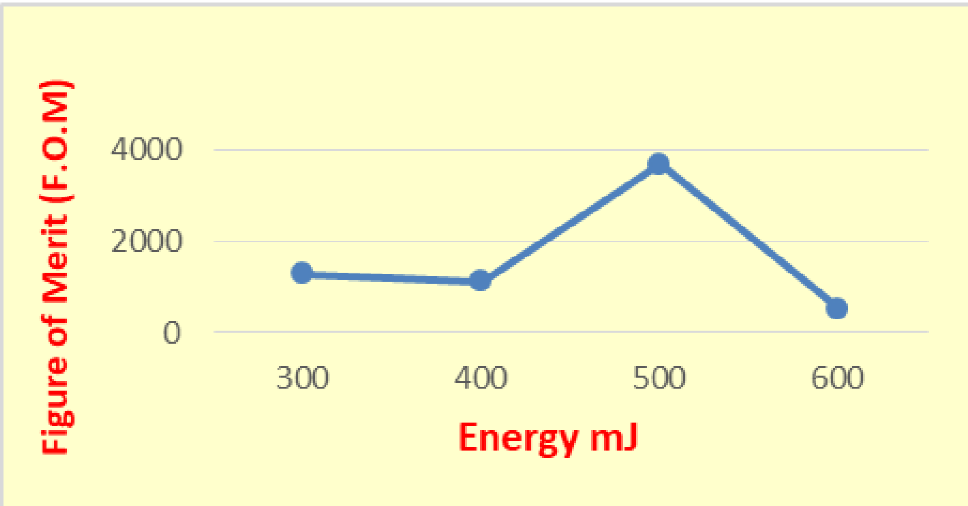


Figure (7). The relationship between Figure of Merit (F.O.M) and laser energies

Table (5). Figure of Merit (F.O.M) measurements of CdO thin films with different energy

| Energy (mJ) | α ($cm^{-1}$) | ϙ (o.cm)$^{-1}$ | F.O.M |
|---|---|---|---|
| 300 | 46273 | 3.62E+01 | 1278 |
| 400 | 40728 | 3.68E+01 | 1106 |
| 500 | 52047 | 1.42E+01 | 3665 |

| | | | |
|---|---|---|---|
| 600 | 16719 | 3.25E+01 | 514 |

### *3-7 $NH_3$ Gas Sensor of CdO as a Function of Time Reaction*

The sensitivity (S %) of pure CdO on a glass substrate at room temperature (RT) was determined to be (17.26, 46.38, and 78.58) ppm of $NH_3$ gas, after which a concentration of (17.26) ppm was fixed million. With temperature changes (50 °C - 150 °C). The time period for opening the gas is (30 sec), starting at (30 sec) and ending at (60 sec). Figure 8 is shown as a function of time with the gas valve on/off. The current increases as the gas level decreases. When a semiconductor is exposed to air, oxygen ions may evolve when electrons are ejected from the band gap and adsorbed on the surface of the semiconductor. If the carrier density decreases, the electron depletion region near the surface will expand, which will greatly reduce the current. When exposed to an $NH_3$ environment, the sensor will register a change in the oxygen species absorbed. $NH_3$ molecules are easily absorbed from the surface because the redox reaction produces little heat. The freed electrons will narrow the depletion area, lowering the semiconductor's resistance. After re-exposing the sensor to ambient air, the adsorbed oxygen species will re-width the depletion area. When the $NH_3$ reaction is finished, the current will revert to its previous value [16].

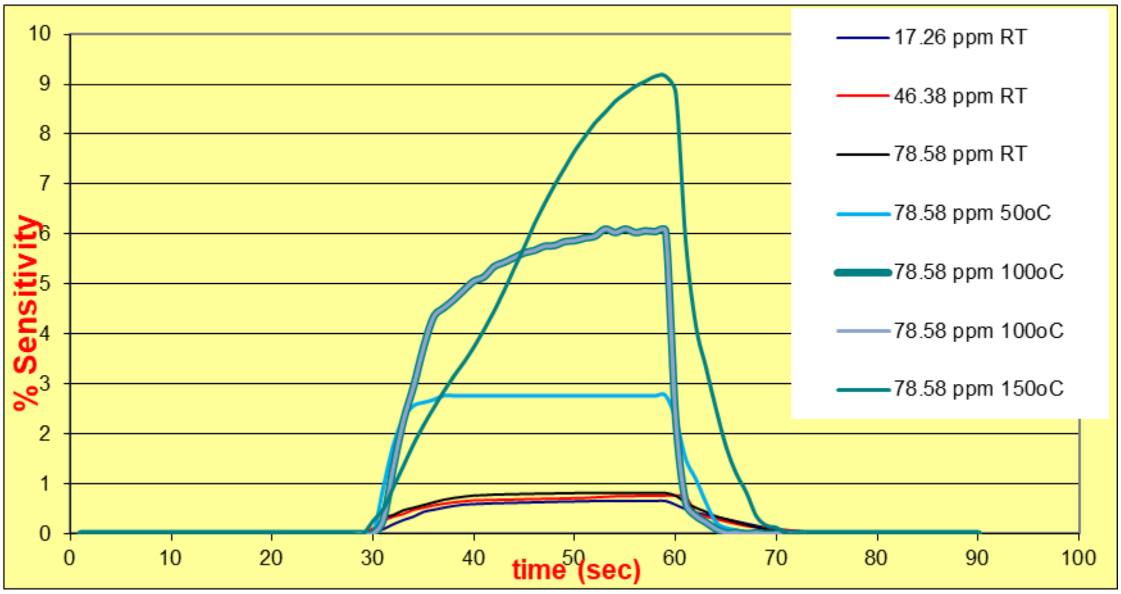


Figure (8). Sensitivity of CdO as a function of time for $NH_3$ gas.

Table (6) explain the sensitivity, response, and recovery values of CdO samples for $NH_3$ s of (17.26, 46.34, and 78.58)ppm at room temperature (RT), and gas concentration (78.58) ppm at a temperature (50, 100, and 150)°C at different reaction times. At room temperature, the sensitivity of CdO films was found to be rather good, and its value increased with increasing reaction time and gas concentration, reaching a value of about (0.82 %) with increasing temperature. As shown in Table (6), the sensitivity increased with increasing temperature until it reached its peak at a temperature value of (150 °C), when it reached (9.2 %) [17].

Table 6. Response time, recovery time, and sensitivity of CdO with various amounts of time

| Concet. (ppm) | Temp. $^oC$ | Seneitivity(%) | SDT | Res. T | Rec.T |
|---|---|---|---|---|---|
| 17.26 | RT | **0.66** | **0.15** | **9.3** | **31.1** |
| 46.38 | RT | **0.76** | **0.18** | **12.8** | **10.3** |
| 78.58 | RT | **0.82** | **0.1** | **8.5** | **9** |
| 78.58 | **50** | **2.8** | **0.12** | **13.6** | **23.8** |
| 78.58 | **100** | **6.1** | **0.05** | **12.8** | **1** |
| 78.58 | **150** | **9.2** | **0.4** | **21.8** | **6.5** |

**4- Conclusions**

In this work, the pulsed laser deposition technique (PLD) was used to form CdO thin films on a glass substrate at varied pulsed laser intensity levels. The X-ray results revealed that the thin films were all polycrystalline and had a hexagonal structure, it can be seen that the film is preferentially oriented along (111) crystallographic directions as well as (200) and (220). This reflects the uniformity of the film material and the relative purity of the target used, and the AFM results demonstrated that increasing the laser power led to an increase in the average diameters and average thicknesses of the deposited films. Measurements of the optical properties found that when the laser power grew, the absorption coefficient increased as well. On the other hand, the energy gap decreases as the laser power increases, but with some difference in the readings; this indicates that the effect of energies is almost convergent, but at energy (600 mJ) there was a clear increase in the film, while FESEM examinations revealed the presence of nanoclusters with an increase in diameter and particle size with increasing energies. The F.O.M chart showed that the optimal energy was (500 mJ). A gas ($NH_3$) gas sensor was constructed, and the effect of increasing gas ratios and temperature on gas sensitivity over time was examined [23].

**5- References**

[1] Gupta, R. K., Ghosh, K., Patel, R., & Kahol, P. K. (2009). Wide band gap Cd0. 83Mg0. 15Al0. 02O thin films by pulsed laser deposition. *Applied surface science*, *255*(8), 4466-4469.
[2] Ali, cadmium dioxide (CdO) nanoparticles prepared by chemical Bath deposition (CBD). *Tikrit Journal of Pure Science*, *27*(5), 76-83.M. Y., Ali, A. Y., & Ali, A. M. (2022). Effects of increasing molar concentration on
[3] Atallah, F. S., Ahmed, H. H., & Jasim, W. K. (2020). Effect of Mg Molar Concentration on Structural and Optical Properties of CdO Thin Films Prepared by Chemical Bath Deposition Method. *Tikrit Journal of Pure Science*, *25*(3), 103-109.
[4] Ilican, S., Caglar, M., Cagar, Y., & Yakuphanoglua, F. (2009). CdO: Al films deposited by sol–gel process: a study on their structural and optical properties. *Optoelectronics & advanced materials-rapid communication*, *3*(2), 135-140.
[5] Aadim, K. A., Ibrahim, A. M. E., & Humaidan, R. M. (2020). Synthesis and Characterization of CdO Nanoparticles Prepared by Pulse Laser Deposition. *Tikrit Journal of Pure Science*, *25*(4), 68-74.
[6] Dakhel, A. A., & Ali-Mohamed, A. Y. (2009). Structural, electrical, and optical absorption properties of LaxCd1− xO solid solution films obtained by sol–gel method. *Materials Chemistry and Physics*, *113*(1), 356-360.
[7] Dakhel, A. A. (2008). Influence of hydrogenation on the electrical and optical properties of CdO: Tl thin films. *Thin Solid Films*, *517*(2), 886-890.
[8] Aadim, K. A., Ibrahim, A. M. E., & Humaidan, R. M. (2020). Synthesis and Characterization of CdO Nanoparticles Prepared by Pulse Laser Deposition. *Tikrit Journal of Pure Science*, *25*(4), 68-74.
[9] Aadim, K. A., & Shehab, M. M. (2021). Influence of Laser Energy on the Structural and Optical Properties of (CdO):(CoO) Thin Films Produced by Laser-Induced Plasma (LIP). *Iraqi Journal of Physics*, *19*(49), 42-52.
[10] Dakhel, A. A., & Ali-Mohamed, A. Y. (2010). Structural and optoelectrical properties of nanocrystalline Gd-doped CdO films prepared by sol gel method. *Journal of sol-gel science and technology*, *55*, 348-353.
[11] Hussain, A. A., Aadim, K. A., & Slman, H. M. (2014). Structural and optical properties of ZnO doped Mg thin films deposited by pulse laser deposition (PLD). *Iraqi Journal of Physics*, *12*(25), 56-61.
[12] Ibrahim, A. M. E., Ahmed, R. H., & Aadem, K. A. (2018). Effect of laser energy on grain size of cadmium oxide nanoparticles in ethanol by PLD method. *Tikrit Journal of Pure Science*, *23*(7), 85-91.
[13] Majeed, Z. N., Al-Samarai, A. M. E., & Mohammed, G. H. (2019). Doping effect by SiO2 on optical properties of ZnO Thin Films Prepared by pulsed laser depositions (PLD) technique. *Tikrit Journal of Pure Science*, *24*(1), 93-97.
[14] Hussain, A. A., Aadim, K. A., & Slman, H. M. (2014). Structural and optical properties of ZnO doped Mg thin films deposited by pulse laser deposition (PLD). *Iraqi Journal of Physics*, *12*(25), 56-61.
[15] Hanfoosh, S. M., & Hassan, N. K. (2019). Optical Properties of Mixed ZnO: Fe2O3 Grown via Pulsed laser deposition. *Iraqi Journal of Science*, 2009-2014.
[16] Sun, P., Zhou, X., Wang, C., Wang, B., Xu, X., & Lu, G. (2014). One-step synthesis and gas sensing properties of hierarchical Cd-doped SnO2 nanostructures. *Sensors and Actuators B: Chemical*, *190*, 32-39.
[17] Wang, C., Yin, L., Zhang, L., Xiang, D., & Gao, R. (2010). Metal oxide gas sensors: sensitivity and influencing factors. *sensors*, *10*(3), 2088-2106.

[18] Shahad, A. D., Hassan, N. K., & Mahmood, Q. H. (2019). Enhancement of ZnO nanostructures Properties Grown by Electrochemical deposition technique. *Tikrit Journal of Pure Science*, *24*(7), 89-92.

[19] Ibrahim, A. M. E., Ahmed, R. H., & Aadem, K. A. (2018). Effect of laser energy on grain size of cadmium oxide nanoparticles in ethanol by PLD method. *Tikrit Journal of Pure Science*, *23*(7), 85-91.

[20] Safah, A. R., Majeed, Z. N., & Mohmood, K. H. (2020). Influence of the Zinc Tin Oxide Nanoparticle proportions on the Optical properties prepared by the laser Method. *Tikrit Journal of Pure Science*, *25*(6), 88-95.

[21] Al-Samarai, A. M. E., Majeed, Z. N., & Mohammed, G. H. (2019). Effect of SiO2 ratio on electrical Properties of SiO2: ZnO Thin Films Prepared by pulsed laser depositions (PLD) technique. *Tik. J. of Pure Sci.*, *23*(10), 76-80.

[22] Ahmed, R. H., Ibrahim, A. M. E., & Aadem, K. A. (2019). Study of the optical proprieties of copper oxide nanoparticles prepared by PLD method. *Tikrit Journal of Pure Science*, *23*(10), 72-75.